

Article

The Influences of Projectile Material and Environmental Temperature on the High Velocity Impact Behavior of Triaxial Braided Composites

Lulu Liu ¹, Shikai Yin ¹, Gang Luo ², Zhenhua Zhao ² and Wei Chen ^{1,*}

- ¹ Aero-Engine Thermal Environment and Structure Key Laboratory of Ministry of Industry and Information Technology, College of Energy and Power Engineering, Nanjing University of Aeronautics and Astronautics, Nanjing 210016, China; liululu@nuaa.edu.cn (L.L.); yinshikai@nuaa.edu.cn (S.Y.)
- ² State Key Laboratory of Mechanics and Control of Mechanical Structures, Nanjing University of Aeronautics and Astronautics, Nanjing 210016, China; mevislab@nuaa.edu.cn (G.L.); zhaozhenhua@nuaa.edu.cn (Z.Z.)
- * Correspondence: chenwei@nuaa.edu.cn

Abstract: Two-dimensional (2D) triaxial braided composites with braiding angle ($\pm 60^\circ/0^\circ$) have been used as aero-engine containing casing material. In the current paper, three types of projectile with the same mass and equivalent diameter, including cylinder gelatin projectile, carbon fiber-reinforced plastics (CFRP), and titanium alloy blade-like projectile, were employed to impact on triaxial braided composites panels with thickness of 4.3 mm at room temperature (20 °C) to figure out the influences of projectile materials on the damage pattern and energy absorption behavior. Furthermore, the influences of environmental temperature were also discussed considering the aviation service condition by conducting ballistic impact tests using CFRP projectile at cryogenic temperature (−50 °C) and high temperature (150 °C). The triaxial braided target panel were pre-heated or cooled in a low-temperature chamber before mounted. It is found that soft gelatin project mainly causes global deformation of the target and therefore absorb much more energy. The triaxial braided composite absorb 77.59% more energy when impacted with CFRP projectile than that with titanium alloy projectile, which mainly results in shear fracture. The environmental temperature has influences on the damage pattern and energy absorption of triaxial braided composites. The cryogenic temperature deteriorates the impact resistance of the triaxial braided composite material with matrix cracking damage pattern, while high temperature condition improves its impact resistance with shearing fracture damage pattern.



Citation: Liu, L.; Yin, S.; Luo, G.; Zhao, Z.; Chen, W. The Influences of Projectile Material and Environmental Temperature on the High Velocity Impact Behavior of Triaxial Braided Composites. *Appl. Sci.* **2021**, *11*, 3466. <https://doi.org/10.3390/app11083466>

Academic Editor: Marta Harničárová

Received: 25 January 2021

Accepted: 7 April 2021

Published: 13 April 2021

Publisher's Note: MDPI stays neutral with regard to jurisdictional claims in published maps and institutional affiliations.



Copyright: © 2021 by the authors. Licensee MDPI, Basel, Switzerland. This article is an open access article distributed under the terms and conditions of the Creative Commons Attribution (CC BY) license (<https://creativecommons.org/licenses/by/4.0/>).

Keywords: impact load; triaxial braided composites; casing containment; damage failure; environmental temperature

1. Introduction

The fan-containment casings of commercial aero-engines, which is a typical thin-walled structure [1], are typically made of two-dimensional (2D) triaxial braided composite materials [2]. To be certified as airworthy, the fan casing must demonstrate that it can resist the impact due to a blade-out event [3]. The application of braided composite materials in aviation thus requires an in-depth investigation of the failure mechanism of these materials under impact loading [4,5].

Verification in the final stages of structural design usually requires full-scale tests and component-level rig tests, which are extremely expensive and require specialized testing equipment [6,7]. Alternatively, ballistic-impact tests on subscale and full-scale components allow designers to optimize the design of composite structures. Numerous ballistic-impact results have demonstrated that target-panel failure is related to the characteristics of both target and projectile, as well as the impact conditions, including the impact velocity and attitude of the projectile. Previous studies [8] also suggest that, under impact loads,

textile composites resist delamination better than laminated composites but exhibit more complicated failure modes. Given that impact behavior is vital to the assessment of aero-engine safety, ballistic-impact tests must be conducted on triaxial braided composites to identify their failure modes and energy-absorption characteristics.

Although numerous efforts have focused on the mechanical properties and failure modes of triaxial braided composites [9–14], a few studies have investigated their impact behavior [15,16]. During impact events, a remarkable strain rate effect at high loading rate is reported in composite materials [17]. In ballistic impact tests, axisymmetric metal projectiles are the most common projectiles used. Sutcliffe et al. [18] used metal projectiles in impact tests of 2D hybrid-glass-carbon-braided composites and found that the damage area increases roughly linearly in impact energy and, for a given impact energy, is greater for lighter impactors. Johnston et al. [19] conducted impact experiments on triaxially braided polymer-matrix composites to study the heat generated in material due to projectile velocity and penetration damage. Note that all the ballistic-impact studies cited above used axisymmetric impactors, such as cylinders or spheres, which facilitates control of the impact attitude. Gelatin projectiles are typical artificial-bird projectiles used for studying issues related to bird strikes [20–23], thus were also used in evaluating. Roberts et al. [24] performed impact tests using cylindrical gelatin projectiles to identify the failure modes of composite plates and half-rings fabricated in a triaxial braided architecture and found that fiber tensile failure occurs in the back ply for both composite plates and half-rings, whereas damage is localized near the impact site as opposed to extending to the boundaries. Such tests using gelatin projectile are designed to induce a high rate of deformation, similar to that experienced by a jet engine fan case during a fan blade-out event. Cheng [25] used gelatin projectiles to examine the impact resistance of a 2D triaxially braided composite panel with different braiding angles and matrix resins, and the impact results were used to validate the proposed methodology, which was called “simplified braiding through-thickness integration points” [26]. Pereira et al. [27] also used gelatin projectiles to measure the impact and high-strain-rate properties of triaxial braided composites and quantified the degradation caused by thermal and hygroscopic aging during service.

Besides gelatin projectiles, a more appropriate impactor for simulating a fractured engine rotor blade is a metallic plate projectile, such as a titanium alloy blade-like projectile [28–32] when investigating the impact resistance of candidate materials for an engine casing. Our previous studies involved blade-containment tests using a high-speed rotor spin tester to investigate the containment and failure mechanisms of a composite casing [33]. Furthermore, to study how projectile shape affects the outcome, we used testing [34,35] and numerical methods [36,37] to compare the impact response and damage evolution of triaxial braided composites for failure events involving blade-like and cylindrical projectiles of the same cross-section perimeter. In addition, Zhao et al. [2] used a plate-shaped titanium alloy projectile in experiments on 2D triaxially braided composites and followed up with numerical parametric studies using a multi-scale finite-element model [38] to examine how projectile deflection angle affects impact failure.

Considering that a carbon-fiber-reinforced fan casing is always accompanied by a composite fan blade [39,40], carbon-fiber-reinforced plastic (CFRP) should also be considered as a potential impactor. Thus, significant benefit is expected from studying the dynamic response of triaxial braided composites impacted by a CFRP projectile and how these impacts differ from those involving metal and gelatin projectiles. However, no research on this subject is yet available in the open literature.

During operation, composite casing is subjected to different ambient temperatures, which may vary from as high as 100–150 °C to as low as –50 °C. Several studies have considered how environmental temperature affects the properties of resin matrix composites, mainly in the case of low-velocity impact. The composite stiffness decreases substantially with increasing temperature, which increases the absorbed energy and peak deflection, causing extensive damage to the specimens [41,42]. Wang et al. [43] experimentally determined the low-velocity impact characteristics of woven carbon-fabric-polyphenylene-

sulfide laminates at 95 and 125 °C. The results reveal that increasing the temperature decreases the stiffness and delamination area and amplifies permanent indentations. Upon increasing the temperature, the failure mechanism transforms from a brittle to a ductile manner. Temperature is closely associated with plastic deformation of the matrix and its coupling with the resin-rich regions and the fiber-bridging mechanism that stems from the specific weave architecture. Khashaba et al. [44] reported that the reduced stiffness and strength is due to softening and plastification of the epoxy matrix, debonding at the fiber-matrix interface, and increased interfacial stress in the re-solidified matrix. Amaro [45] investigated how temperature affects the multi-impact performance and reported that the number of impacts to failure depends strongly on the temperature because of the global properties of the matrix.

The effect of low temperature on triaxial braided composites is another rarely studied subject. Sreekantha et al. [46] carried out low-velocity impact experiments on E-glass-epoxy composite laminates at both sub-zero and elevated temperatures, and the results indicate that temperature more strongly affects the perforation threshold energy of thicker laminates because of increased laminate rigidity at low temperature. Ma et al. [47] investigated how glass-fiber-reinforced polymer composites respond to low-velocity impact under cryogenic conditions. Finally, Shimamoto et al. [48] performed high-speed impact experiments on CFRP at cryogenic temperatures. However, no studies have yet reported how environmental temperature affects the impact response of triaxial braided composites, which poses a threat to the safety of aero-engines.

From the above analysis, it can be seen that there are still two challenges in the safety research of aero-engine 2D triaxial braided composite casing. First of all, the fly-off blades may be made of composite materials or titanium alloys, and there is no corresponding testing data or analysis on the containment capability of the casing to blades made of completely different materials. Second, the influence of the service environment temperature of the 2D triaxial braided composite casing on its containment capability is still unclear, which threaten the aviation flight safety. The present work uses three types of projectiles, cylindrical gelatin projectiles, CFRP blade-like projectiles, and titanium alloy blade-like projectiles, in ballistic-impact tests to identify the damage pattern and failure modes of 2D triaxial braided composites. These ballistic-impact tests were conducted at both low and high temperatures. We study how projectile material and environmental temperature affects the damage pattern and energy absorption of the composites, which should provide the basic concept to design impact-resistant fan components for aero-engines.

2. Ballistic Impact Test

2.1. Test Specimen

The composite target was braided with 12k T700 carbon fiber in the form angle of ($\pm 60^\circ/0^\circ$). Figure 1 shows the process for manufacturing triaxial braid composites: First, a triaxial braider, mounted with the axis horizontal, created a braid tube using 12k flat tow fibers in both the $\pm 60^\circ$ (bias) and 0° (axial) directions (Figure 1a). The tube was then flattened into a double-walled tape (Figure 1b). Next, the three layers of flattened tapes were piled up with the 0° fibers aligned. Triaxial braided composite panel was fabricated using the resin-transfer molding technique, whereby epoxy resin was infused into multiple layers of dry braided preform. This transfer molding method has the advantages of good surface finish, dimensional stability, and good mechanical properties [49]. The fiber volume was the same in each direction so that both the individual plies and the entire lay-up were quasi-isotropic. From a large panel, 250 mm \times 250 mm composite targets were cut out, each 4.3 mm thick.

As mentioned in the Introduction part, there are three types of projectiles which are commonly used or have potential application for fan blade out events of aero-engine, i.e., cylindrical gelatin projectiles, rectangular titanium alloy projectiles, and composite blade-like projectiles. In the current study, these three projectiles were designed with the same mass. The geometry and dimensions of three types of projectile were shown in

Figure 2. The gelatin projectiles were shaped as flat-ended cylinders with 30 mm diameter and 52 mm height. The cylindrical gelatin projectile has a density of 950 kg/m^3 and a porosity of 10%. The CFRP and titanium-alloy projectiles were both rectangular, 70 mm long, and 40 mm wide. Considering the differences in density, the CFRP projectile was 6 mm thick while the titanium-alloy projectile was 2 mm thick. Because the current research is aimed at a specific engine containing casing as the research object, the design of the projectile is based on the engine rotor blades, which is usually a thin sheet with a three-dimensional twisted blade shape. Therefore, the thickness of 2 mm of the titanium alloy blade herein is a suitable thickness. The thickness of the CFRP material body is determined based on the density difference between the titanium alloy material and the carbon fiber composite material. The CFRP projectile is a 12-layered woven fabric-reinforced laminate. The rectangular projectiles have the same equivalent diameter as the gelatin cylinder.

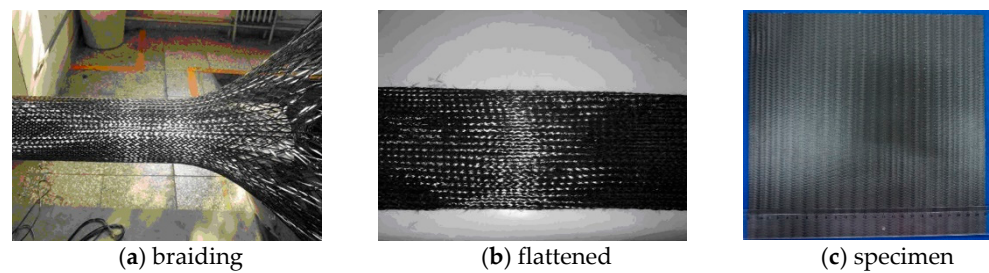


Figure 1. Processing of two-dimensional triaxial carbon fiber braided composites.

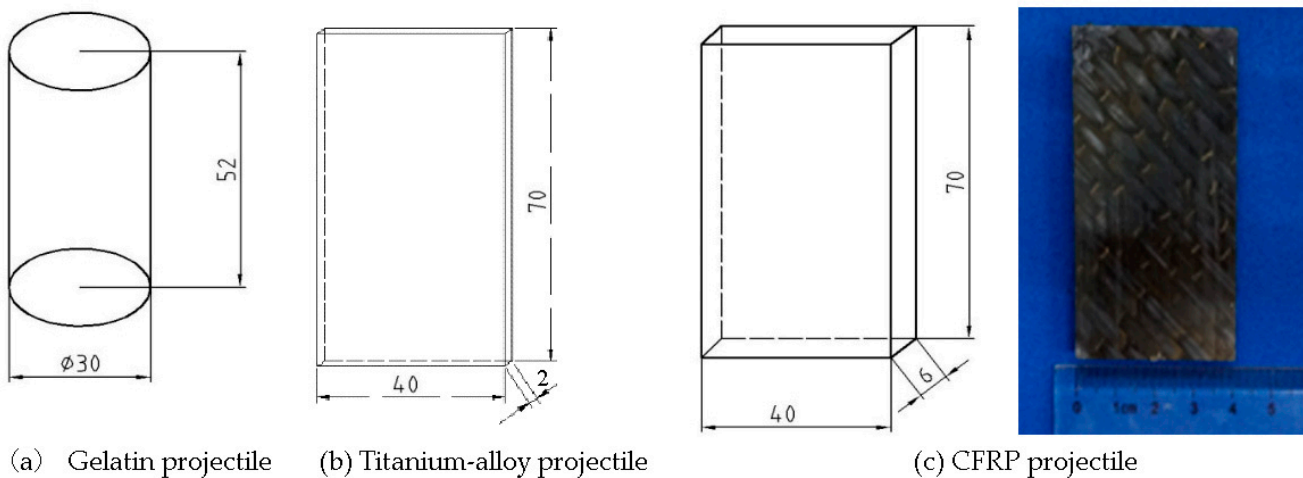


Figure 2. Size and shape of the different types of projectiles.

2.2. Testing Device

The 65-mm-caliber gas gun used in the ballistic tests accelerated the projectile to a maximum velocity of 200 m/s. Figure 3 shows the principle diagram and structural drawing of this single-stage gas gun. The projectile is supported by foam in an aluminum sabot. The sabot and projectile are pushed and accelerated by compressive air in the gun barrel. The projectile launch velocity is varied by changing the air pressure. The sabot is captured at the exit of the gun barrel by a sabot separator while the projectile moves forward and impacts the target directly. The spallation fragments from the target, projectile with residual velocity, and foam fragments are arrested by the fragment collector mounted on the back of the target.

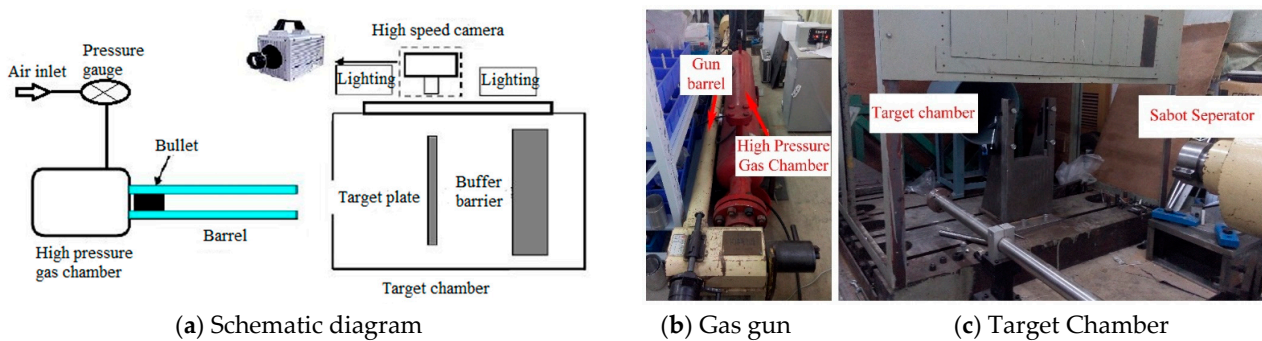


Figure 3. Schematic diagram of ballistic-impact testing device with gas gun system.

2.3. Testing Methods

The actual projectile impact velocity was measured by a velocimetry system installed between the gun muzzle and the target because it runs independently and has high accuracy. As a projectile passes through the velocimetry system, successive laser beams are obstructed, generating corresponding voltage signals. Given the time interval between two trigger signals and the distance between laser beams in the velocimeter, the velocity is determined. In the actual process, fragments such as foam in the sabot may interfere with the measurement of the velocimeter, so the speed of each test was checked by high-speed photography. Furthermore, the muzzle is very close to the target to reduce the flight distance of the projectile, thereby reducing the speed change and attitude change during the flight of the projectile, so as to improve the test accuracy.

Figure 4 shows how the specimens were mounted. Unlike the usual axisymmetric projectile, the blade-like projectile is shaped, making it difficult to control its impact posture. In the present research, the projectile was fixed in an aluminum alloy sabot with four V-shaped grooves at the front edge. When the sabot was captured by the sabot separator, a petal-shaped tear forms and dissipates the kinetic energy of the sabot. The triaxial braided composite plate is fixed along both the short edges using four bolts, leaving the upper and lower edges free. A high-speed camera, MEMRECAM HX-7 (NAC cooperation) is fixed through the bracket above the impact plane to take photos at a frame rate of 3000 frames per second. These high-speed photos are designed to image the target during projectile trajectory and deformation. They also serve to estimate the residual velocity of the projectile for the given perforation conditions.

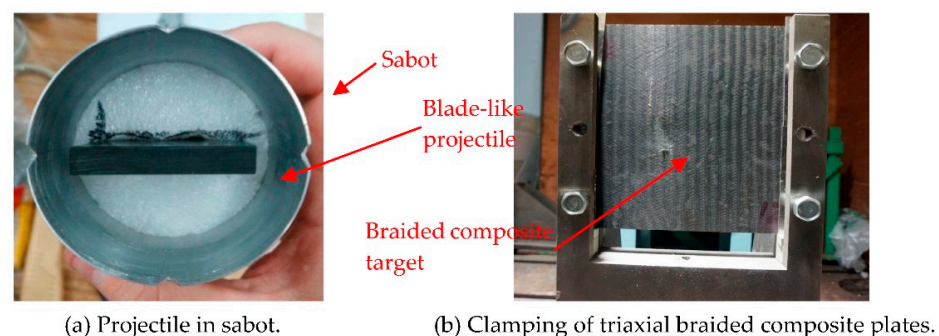


Figure 4. Mounting of specimen under test.

Considering that the triaxial braided composite casing using in aero-engine could be subjected to different ambient temperatures, varying from as high as 100~150 °C to as low as −50 °C. To figure out the influences of environmental temperature during service, we also conducted a series of impact tests of a 2D triaxial braided composite target plate at high temperature (150 °C) and cryogenic temperature (−50 °C). For the high-temperature tests, the composite target was heated at 2 °C/min to a predetermined temperature (155 °C) in an electric blast oven, following which the target was thermally insulated for half an hour to

allow the homogenization of the internal temperature of the composite target. The heated target was removed from the insulation and immediately installed in the target holder. For the tests at cryogenic temperature, the target was cooled in a low-temperature chamber filled with dry ice (a solid form of carbon dioxide with a sublimation point of $-78.5\text{ }^{\circ}\text{C}$). Dry ice sublimates at normal temperature and pressure, absorbing a large amount of heat from the environment and thereby decreasing the surrounding temperature. The composite target was placed in the cryogenic chamber for 2~3 h and then immediately installed in the target holder. When installing, the bolts are installed with a constant torque wrench with a constant value. Compared with directly on the target plate clamping system, the design of this heating and cooling method could make the clamping pressure of the target plate not change at room temperature, high temperature, and low temperature, thereby exert no interfere with the results. The actual temperature of the target was measured using an infrared thermometer. For both high- and low-temperature tests, the projectile was launched immediately after installing the target in the target holder, and the high-speed camera was triggered to capture images.

3. Results and Discussion

3.1. Influence of Projectile Material

Table 1 shows the results of high-speed impact tests on 2D triaxial braided composites using different types of projectiles at room temperature ($20\text{ }^{\circ}\text{C}$). In the impact analysis, the ballistic performance is normally measured by energy absorption. Energy absorption of composites is defined as the consumption of kinetic energy of the projectile. For cases that projectiles rebound, it is considered as the total kinetic energy of the projectile is absorbed by fabric targets. According to the initial velocity and residual velocity, the energy absorption of fabrics can be calculated as:

$$E_{absorbed} = \begin{cases} \frac{1}{2}mV_i^2 & \text{(Rebound)} \\ \frac{1}{2}m(V_i^2 - V_r^2) & \text{(Perforation)} \end{cases} \quad (1)$$

in which m denotes the projectile mass, V_i denotes the initial velocity of the projectile, and V_r denotes the residual velocity of the projectile.

Table 1. Results of high-speed impact tests of triaxial braided composites with projectiles made of various materials at room temperature.

| Testing Number | Projectile Weight m (g) | Impact Velocity V_i (m/s) | Residual Velocity V_r (m/s) | Testing Results | Energy Absorption E_a (J) | Average Energy Absorption (J) | Standard Deviation (J) |
|----------------|---------------------------|-----------------------------|-------------------------------|--------------------------|-----------------------------|-------------------------------|------------------------|
| Gelatin-1 | 25.6 | 169 | – | Projectile fragmentation | 365.58 | – | – |
| Gelatin-2 | 27 | 213 | – | Projectile fragmentation | 612.48 | | |
| Ti-1 | 25 | 105 | 23 | Perforation | 131.2 | 150.4 | 22.58 |
| Ti-2 | 24.3 | 146 | 83 | Perforation | 175.29 | | |
| Ti-3 | 24.8 | 160 | 118 | Perforation | 144.78 | | |
| CFRP1 | 27.8 | 118 | 0 | Rebound | 193.54 | 267.1 | 24.38 |
| CFRP2 | 27.3 | 131 | 0 | Rebound | 234.25 | | |
| CFRP3 | 26.1 | 157 | 45 | Perforation | 295.24 | | |
| CFRP5 | 27.1 | 170 | 101 | Perforation | 253.37 | | |
| CFRP6 | 28.2 | 172 | 108 | Perforation | 252.67 | | |

Two sets of impact tests were performed with cylindrical gelatin projectiles: one with a projectile velocity of 169 m/s and another with a projectile velocity of 213 m/s. However, even with an impact velocity as high as 213 m/s, the triaxial braided composites were not perforated by the gelatin projectile. On the contrary, the gelatin projectile flows and fragments during impact. We thus deduce that the ballistic-limit velocity is greater than 213 m/s. As the gelatin projectile flow away after impact, the residual velocity could not be obtained, therefore the energy absorption is not available.

Three sets of impact tests were carried out using titanium-alloy blade projectiles and impact velocities ranging from 105 to 160 m/s. In all three sets of tests, the titanium-alloy projectile perforated the target plate, indicating that the ballistic-limit velocity is below 105 m/s for a titanium-alloy projectile.

Six sets of tests were carried out using the CFRP projectiles. In two sets of tests, the projectile rebounded, whereas the projectile perforated the target in the four remaining sets of tests. At impact velocities of 118 and 131 m/s, the target was not perforated, and the CFRP projectile rebounded. At higher impact velocities, 157~172 m/s, the 2D triaxial braided composite targets suffered damages of a similar pattern. The triaxial target is perforated by the CFRP projectile at 157 m/s, but not at 131 m/s, so the ballistic limit is between these two velocities.

Based on this analysis, the triaxial braided composite target plate has significantly different ballistic-limit velocities for the three types of projectiles made of different materials but of similar mass and equivalent diameter. The ballistic-limit velocity of the CFRP, gelatin, and titanium-alloy projectile is between 131 and 157 m/s, above 213 m/s, and below 105 m/s, respectively. The target has the highest ballistic limit for the gelatin projectile, followed by the composite material blade-like projectile, and then by the titanium-alloy metal projectile with the lowest ballistic-limit velocity.

3.1.1. Energy Absorption

Figure 5 shows the energy absorbed by 2D triaxial braided composites as a function of impact velocity, and Figure 6 shows the energy absorbed by the composite target when impacted by projectiles made of various materials. The composite target absorbs the most energy (>612.5 J) when impacted by the gelatin projectile. Because the composite target was not perforated by this projectile at any of the velocities tested, still more energy can be absorbed by this material. When the composite target was impacted with CFRP and titanium-alloy blade-like projectiles, the energy absorption of the composite target first increases and then decreases with increasing impact velocity. When the triaxial braided composite was perforated by a CFRP projectile, the average energy absorbed is 267.1 J, which is 77.59% greater than the maximum average energy absorbed of 150.4 J for a titanium-alloy projectile. According to the study by Anderson Jr. et al. [50], the ballistic limit velocity decreases significantly with the increase in projectile hardness after the projectile hardness exceeds that of the target. In the current study, the composite target and CFRP projectile has moderate hardness while the titanium projectile has obviously greater hardness than the target panel. Therefore, the ballistic limit velocity as well as energy absorption decreases when used titanium alloy projectile. It is worth noting that the previous research on the hardness of the projectile was generally in the field of metal materials. The projectile studied in the current research has a larger material span, ranging from soft gelatin to resin-based composite materials to metal alloy materials.

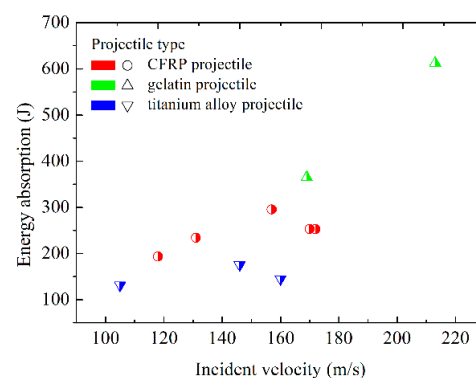


Figure 5. Energy absorption of two-dimensional (2D) triaxial braided composites with incident velocity of projectile.

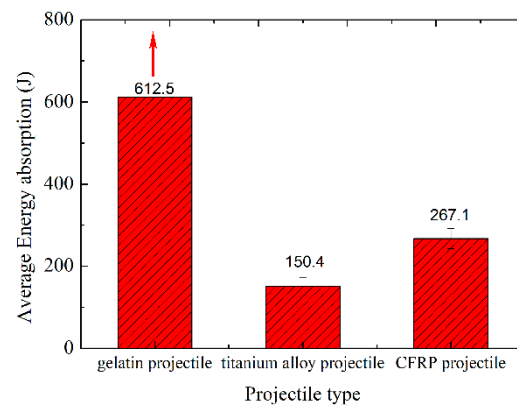


Figure 6. Energy absorption of 2D triaxial braided composites impacted by various projectiles.

For both titanium-alloy and CFRP projectiles, first, the energy absorption increases with the incident velocity, and then, it decreases when the incident velocity exceeds a critical value. This phenomenon is widely observed in ballistic impact, whether it is a metal target plate or a composite material target plate.

3.1.2. Impact Process

High-speed cameras were used to record the impact by various types of projectiles on a braided composite target. Figure 7 shows the impact of a gelatin projectile in the Gelatin-2 test. As the impact velocity is extremely high in the tests using gelatin projectile, the gelatin projectile deformed and failed to maintain its original cylindrical geometry. The deformation phenomenon of gelatin projectile was investigated in our recent study [51] and corresponding internally supported gelatin bird projectile were used to improve this undesirable deformation. It is found that the deformed gelatin projectile mainly affects the load characteristic. Considering the flow characteristic of gelatin projectile during impact, the deformation of the gelatin projectile before impact has limited influence on the damage features of the composite target. Therefore, the gelatin projectile could be comparable with other projectile.

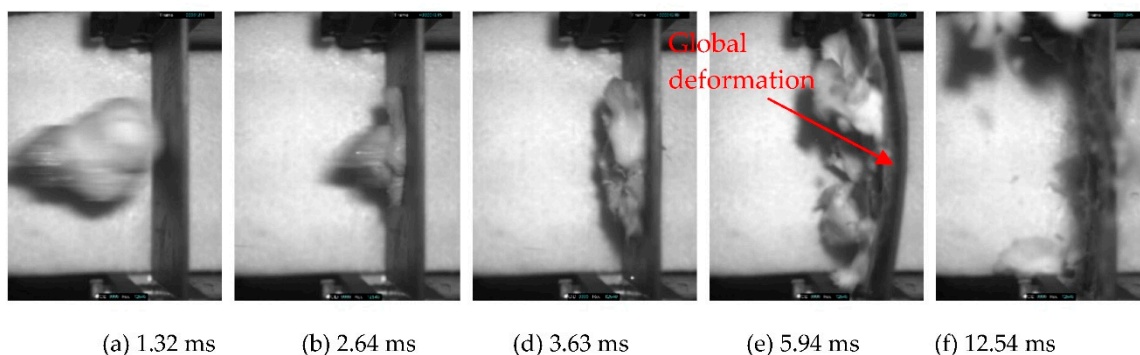


Figure 7. High-speed photographs of impact on 2D triaxial braided composite target plate of gelatin projectile at an impact velocity of 213 m/s.

The cylindrical gelatin projectile first contacts the target at 1.32 ms and undergoes a significant flow during the impact, which is fully consistent with reports in the literature. The triaxial braided composite target undergoes a large bending deformation under the impact of the gelatin projectile, which absorbs the impact energy to a large extent. Finally, the composite target plate is not perforated by the gelatin projectile, and the target plate recovers completely from the bending deformation. The large bending deformation of the target during impact results in delamination and matrix cracking of the target. Since the

gelatin projectile is less hard than the carbon-fiber composite target, the target suffers no significant fiber breakage.

Figure 8 shows the impact of the titanium-alloy projectile perforating a 2D triaxial braided composite target in the Ti-1 test. The projectile is in an ideal posture before hitting the target plate. The contact with the target plate begins at 5.28 ms. At 12.21 ms, about 2/5 of the length of the blade projectile has passed through the target, and, at 21.12 ms, the titanium-alloy projectile completely passes through the target. During the entire impact of the titanium-alloy blade projectile, the target plate undergoes limited bending deformation, which differs significantly from the case for impact by the gelatin projectile. This also explains the concentrated damage inflicted on the target plate and the low energy absorbed.

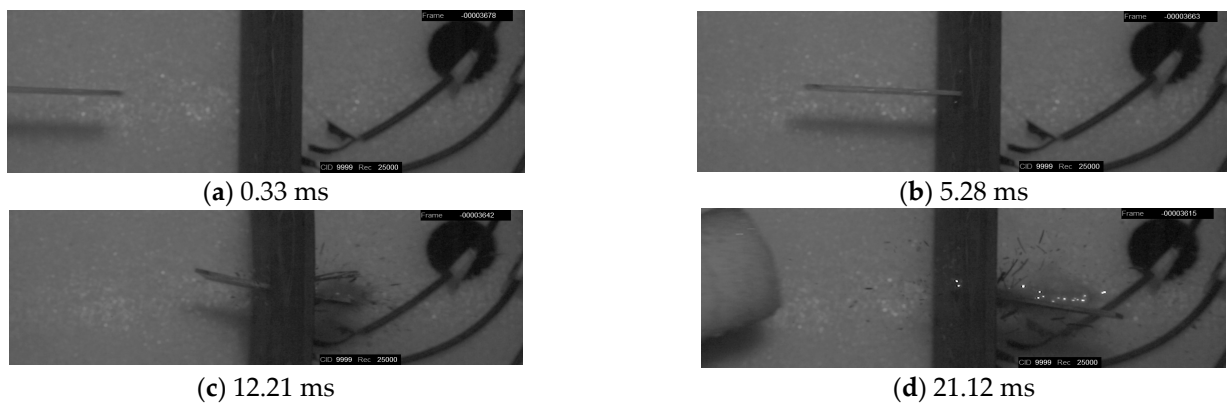


Figure 8. High-speed photographs of impact on 2D triaxial braided composite target plate of titanium-alloy projectile with an impact velocity of 105 m/s.

Figure 9 shows the process of CFRP projectiles perforating a 2D triaxial braided target in a CFRP-3 test. At 0.42 ms, the CFRP projectile makes initial contact with the target plate, and, at 1.05 ms, it has almost passed through the target plate. The target plate undergoes no obvious bending deformation during the impact, and material is ejected from the back of the target plate due to matrix fragmentation.

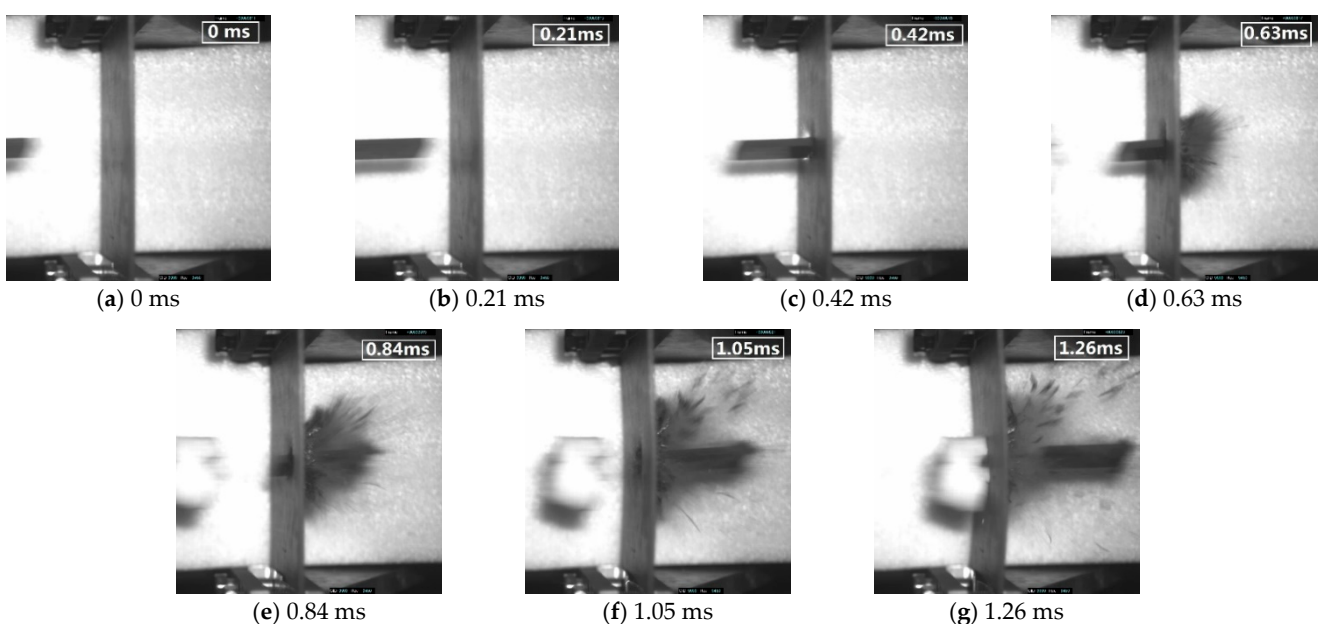


Figure 9. Perforation of 2D triaxial braided composite target plate by carbon fiber-reinforced plastics (CFRP) projectile with impact velocity of 157 m/s (CFRP-3 test).

3.1.3. Damage Morphology

The triaxial braided composite target plate suffers no visible damage on the impact surface when impacted with a gelatin projectile at an impact velocity of 169 m/s. Figure 10 shows the morphology of the damage suffered by the target after the impact of the gelatin projectile at an impact velocity of 213 m/s. The impact surface reveals no obvious deformation or fiber breakage. However, delamination, matrix cracking, and a small amount of fiber breakage appears in the through-thickness direction of the target. The damage to the exit surface of the target plate is indicative of matrix cracking at a distance from the impact point. The boundary conditions of the composite panel affect the dynamic response and deformation features of the target panel, correspondingly resulting in different damage patterns. Therefore, if clamping in all edges, it is possible to obtain the results of perforation by the gelatin projectile, as illustrated in literature [24].

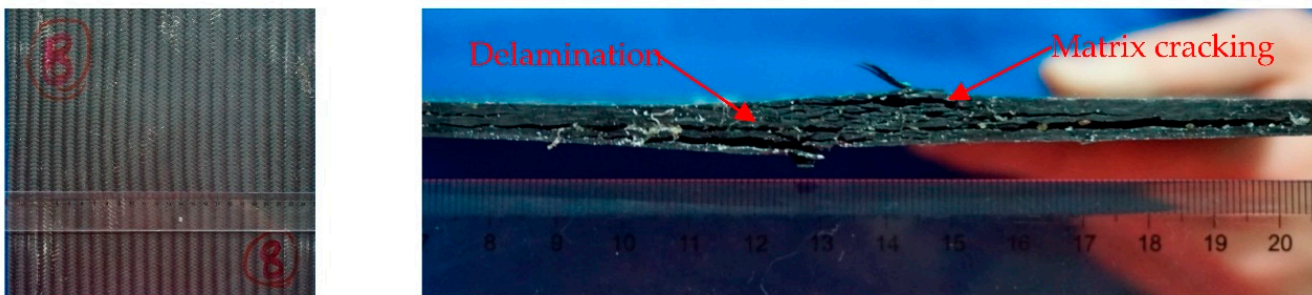


Figure 10. Damage to 2D triaxial braided composite target plate caused by impact of gelatin probe. (Gelatin-2 test, 213 m/s).

Although the gelatin projectile did not perforate the target, the existing test results have fully proved that the energy absorption of the composite material panel is much higher when impacted with soft gelatin projectile than that with the hard metal and composite material. The main reason for this result is that, due to the fluid behavior of the gelatin projectile during impact, the contact area with the target plate during impact is much larger than the impact area of the metal and composite blade-like projectiles. The target plate undergoes an overall large bending deformation, which dissipates more impact energy. Consequently, the impact energy is more evenly distributed over the entire target plate.

Figure 11a shows the morphology of the damage suffered by the 2D triaxial braided composite target in the Ti-1 test due to the impact of a titanium-alloy projectile at an impact velocity of 105 m/s. A significant shear fracture rectangular opening appears on the incident surface, with an area and shape that are substantially the same as the cross-sectional area of the titanium-alloy projectile, which was quite small and thin. On the exit surface of the target appears an elliptically bulged area of damage. The damaged area shows obvious damage modes such as fiber breakage, matrix cracking, or delamination, as shown in Figure 12. Figure 11b shows the damage of a 2D triaxial braided composite after impact by a titanium-alloy projectile at an impact velocity of 160 m/s (Ti-3 test). Given that the blade projectile has a certain yaw angle when it exits, an open-type tear occurs on the incident surface of the projectile. The damage on the backside of the target plate is more serious: the damage area is about twice that of the incident-projectile surface, and obvious fiber breakage and delamination have occurred.

The test results show that, for the titanium-alloy projectile perforating the 2D triaxial braided composite target plate, the damage form and damage mode of the target plate are basically the same (i.e., fiber shear fracture and local matrix cracks on the impact surface, and bulged deformation with fiber breakage, fiber pull-out, and delamination). The damage area is smaller.

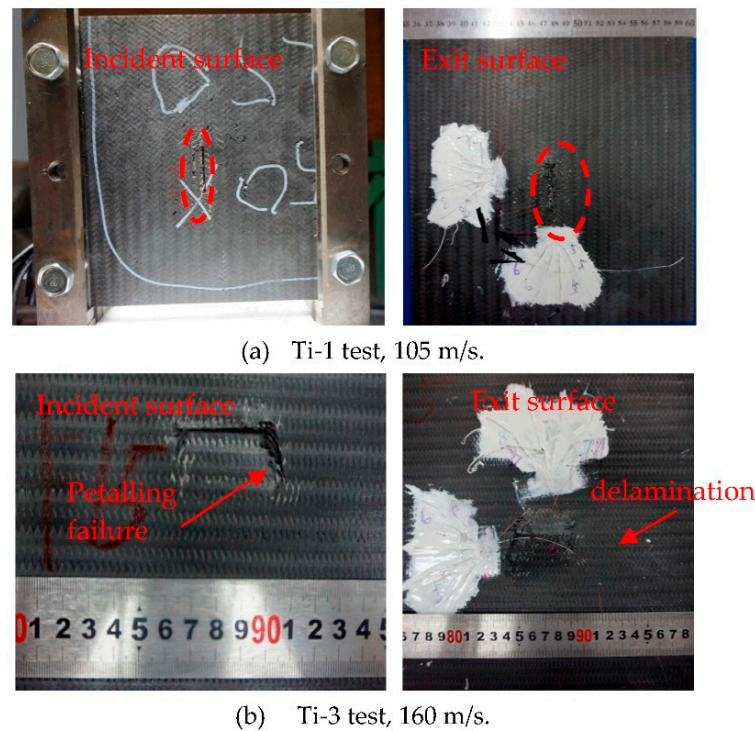


Figure 11. Damage to 2D triaxial braided composites impacted by titanium-alloy projectile.

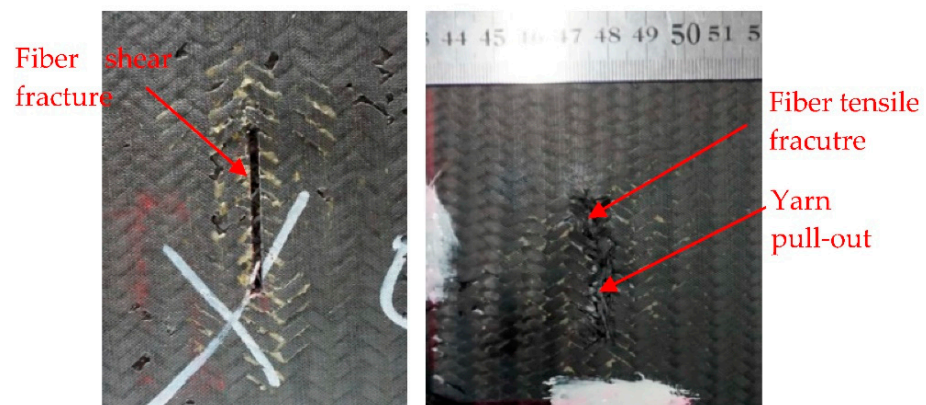
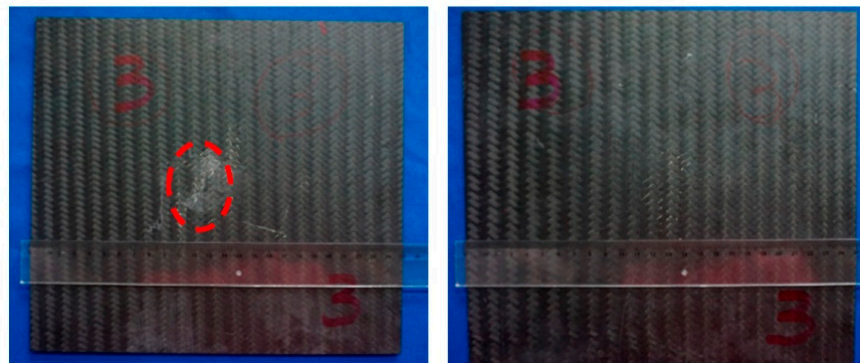


Figure 12. Local damage patterns of 2D triaxial braided composites impacted by titanium-alloy projectile.

In rebound cases, the typical damage caused by the CFRP projectile on the front side of the target is relatively similar. As shown in Figure 13a, projectile impact creates a rectangular sunken area of the same size as the cross-section of the projectile. The sunken area is shallow, with no visible cracking or damage. No visible matrix cracking, bending deformation, or serious delamination appears on the exit surface of the triaxial braided target. The target plate remains basically intact with no visible damage. Figure 13b shows the damage to a triaxial braided composite target after perforation by a CFRP blade-like projectile with an impact velocity of 157 m/s. The damage area is relatively centralized with a rectangular perforative opening at the impact point. The area of the perforative opening is slightly larger than the cross-section of the CFRP projectile. The damage area on the impact surface surrounds the perforative opening and consists of slight damage and a certain degree of cracking and delamination. At the exit surface, the damage to the braided composite is much more serious and consists of massive fiber breakage, yarn pull-out, severe matrix cracking, and delamination in the bulged broom area.



(a) CFRP-2 test, $V_i = 131.1\text{m/s}$, room temperature.



(b) CFRP-3 test, $V_i = 157\text{ m/s}$, room temperature.

Figure 13. Impact damage to 2D triaxial braided composite targets caused by impact of CFRP projectile: (left) incident surface, (right) exit surface.

For perforation with various impact velocities, the morphology of the damage to the 2D triaxial braided composite target plate is of a similar pattern, although with a different extent of damage. A rectangular opening with an area of shear damage and local matrix cracking appears on the impact surface. In addition, a local bulge deformation area appears with fiber breakage and delamination, and the main failure modes in the damaged area are fiber tensile failure, yarn pull-out, matrix cracking, and delamination.

From the analysis above, the target plate absorbs the least energy upon impact of the titanium-alloy blade projectile. The main reason for this result is that the titanium-alloy blade projectile is the hardest of the projectiles and has the smallest cross-sectional area for the impact surface. Therefore, when a titanium-alloy projectile impacts the composite target, the target plate is damaged in a shear pattern, which hinders the target plate in dissipating energy through a bending deformation. In addition, a shorter projectile-target interaction time means that the target plate has insufficient time to deform. As a result, the damage area of the target plate is also small.

3.2. Impact Characteristics under Cryogenic and High Temperatures

Based on the research detailed above, the CFRP projectile produces ballistic impacts on triaxial braided composites at cryogenic and high temperatures that most closely resemble the ballistic impacts in real engines. Table 2 presents the results of ballistic-impact tests at cryogenic and high temperatures, where “C” refers to cryogenic conditions, and “H” refers to high-temperature conditions.

Table 2. Results of high-speed impact test of triaxial braided composite under high (H) and cryogenic (C) temperatures.

| Test Number | Temperature T (°C) | Projectile Weight (g) | Initial Velocity V_i (m/s) | Residual Velocity V_r (m/s) | Result | Energy Absorbed E_a (J) | Average Energy (J) | Standard Deviation (J) |
|-------------|--------------------|-----------------------|------------------------------|-------------------------------|-------------|---------------------------|--------------------|------------------------|
| C1 | −49.9 | 27.8 | 70.5 | −22.7 | Rebound | 61.92 | 189.3 | 22.36 |
| C2 | −47.2 | 26.7 | 130 | 62.5 | Perforation | 173.47 | | |
| C3 | −47.5 | 27.2 | 147 | 80.8 | Perforation | 205.09 | | |
| H1 | 139.5 | 26.9 | 130 | − | Rebound | 227.31 | 276.7 | 26.52 |
| H2 | 143 | 28.3 | 146 | −45.5 | Rebound | 272.33 | | |
| H3 | 149 | 27.3 | 170 | 100 | Perforation | 257.98 | | |
| H4 | 149.5 | 27.4 | 185 | 112.5 | Perforation | 295.49 | | |

At cryogenic temperature, the triaxial braided composite target is perforated at 130 m/s, whereas the projectile rebounds at 131.1 m/s at room temperature. At high temperature, the triaxial braided composite target is perforated at 170 m/s, whereas the projectile rebounds at 146 m/s. Based on these results, we deduce that the ballistic-limit velocity is highest at high temperature, followed by the room temperature and then low temperatures. In other words, cryogenic temperatures decrease the impact resistances of the triaxial braided composites, whereas high temperatures increase their impact resistance. Differences between the impact resistance and forms of damage under these three temperature ranges is discussed in detail below based on the test results.

3.2.1. Energy Absorption

To further study the energy absorption by triaxial braided composite materials due to the impact of CFRP blade projectiles at various temperatures, Figures 14 and 15 show the energy absorbed as a function of impact velocity for various temperatures and the average energy absorbed at three temperatures, respectively. Significantly less energy is absorbed by the triaxial braided composite plate at cryogenic temperatures than at room temperature or high temperature. At cryogenic temperatures, the average energy absorbed in cases of target perforation is 189.3 J, which is 22.4% less than at room temperature. The average energy absorbed at high temperature, on the contrary, increases by 13.4% with respect to that at room temperature. These results indicate that low temperature degrades the impact resistance of the two-dimensional triaxial braided composite material, whereas high temperature improves its impact resistance.

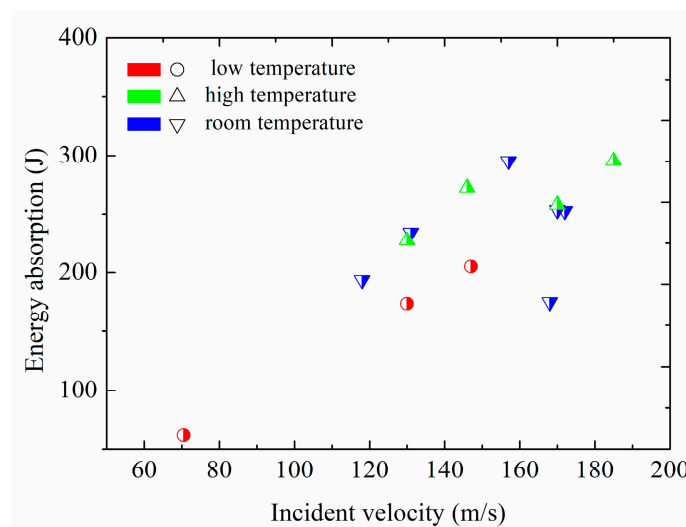


Figure 14. Energy absorbed by 2D triaxial braided composite targets as a function of impact velocity and for three different temperatures.

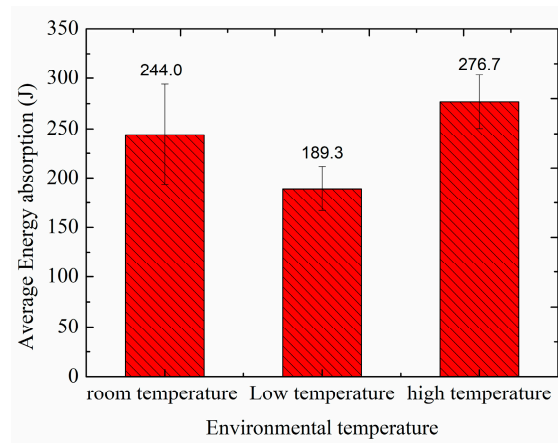
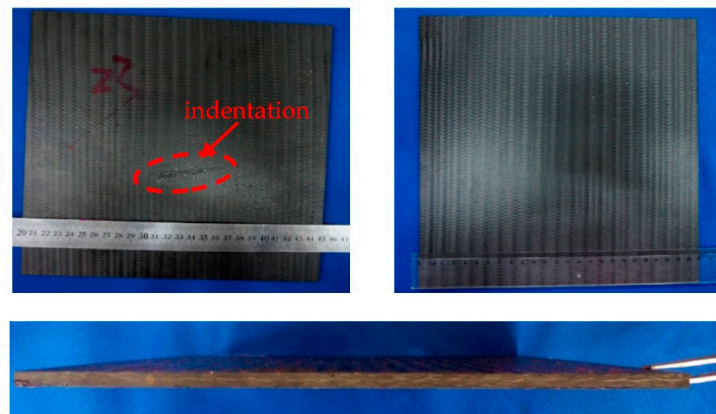


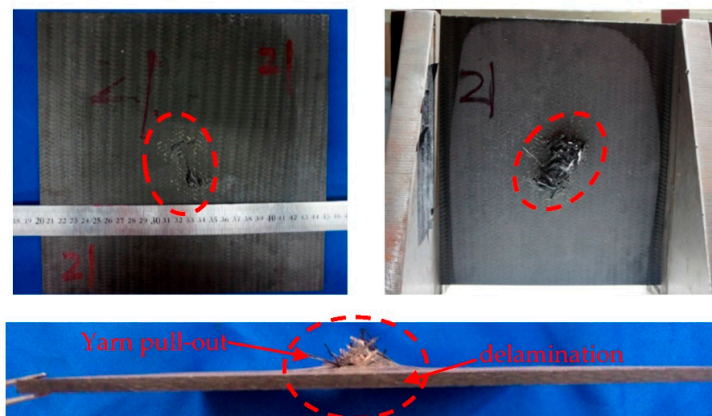
Figure 15. Energy absorbed by 2D triaxial braided composite target at various temperatures.

3.2.2. Damage Morphology

With the target plate at cryogenic temperature, three impact tests were undertaken using the composite projectile. The projectile perforated the target plate in tests C2 and C3 (see Table 2), and the projectile rebounded in test C1. Figure 16 shows the damage morphology, where the left-hand images show the damage at the impact surface of the target, and the right-hand images show the damage at the exit surface. The picture at the bottom shows a cross-sectional view of the damage.



(a) C1, $V_i = 70.5 \text{ m/s}$, $T = -49.9 \text{ }^\circ\text{C}$.

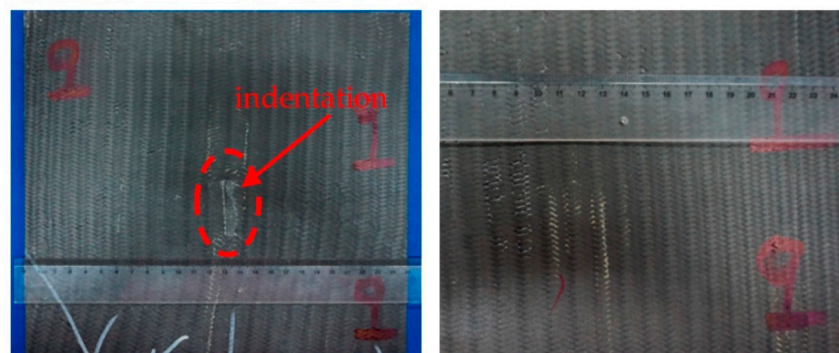


(b) C3, $V_i = 147 \text{ m/s}$, $T = -47.5 \text{ }^\circ\text{C}$.

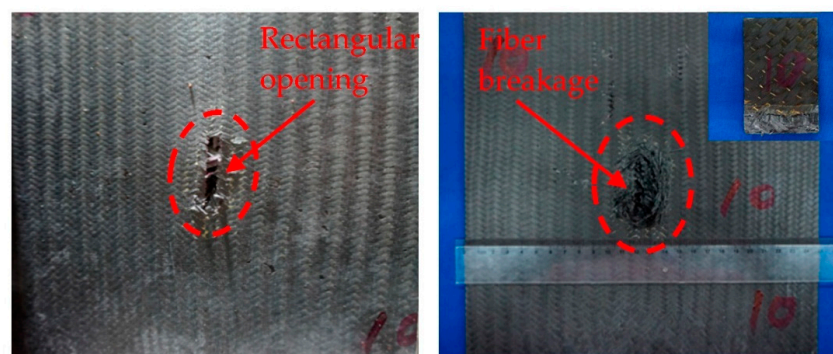
Figure 16. Damage to 2D triaxial braided composites at cryogenic temperature.

Figure 16a shows damage caused by test C1, in which the projectile failed to perforate the target. In this case, the projectile caused relatively little damage to the target. Only a slight crater appears due to the shearing action of the projectile at the impact surface, whereas no visible damage appears at the back surface of the target. We deduce from these results that the impact velocity is far below the ballistic limit. When the composite target plate is perforated, a strip opening appears on the incident surface that matches the size of the rectangular projectile. At the exit surface of the target, a wide-ranging, elliptically shaped, broom-like damage area appears, and yarn fracture and delamination are evident. In the C3 test (with a larger incident velocity), more severe crack growth appears at the two ends of the perforation strip, and the damage crack is also significantly larger than that of the C2 test.

A total of four ballistic-impact tests were performed at high temperature. In tests H3 and H4 (see Table 2), the projectiles perforated the target. Figure 17 shows the damage morphology for tests H2 and H4. In tests H2 (impact velocity of 146 m/s) and H1 (impact velocity of 130 m/s) tests, the projectile failed to perforate the target but rebounded. As for the tests under cryogenic conditions, rectangular craters of various depths appear on the impact surface of the target. The crater depth of the H2 target (for a larger impact velocity) significantly exceeds that of the H1 test. Therefore, we consider that, under conditions of rebound, the depth of the impact crater increases with increasing impact velocity. When the target was perforated in tests H3 (impact velocity of 170 m/s) and H4 (impact velocity of 185 m/s), a clear, neat strip perforation was produced on the front surface of the target, corresponding to the shape and size of the projectile, and clear cracking and delamination appeared on the exit surface. In addition, when the projectile impacts the target plate, the projectile itself also suffers fiber breakage and delamination failure.



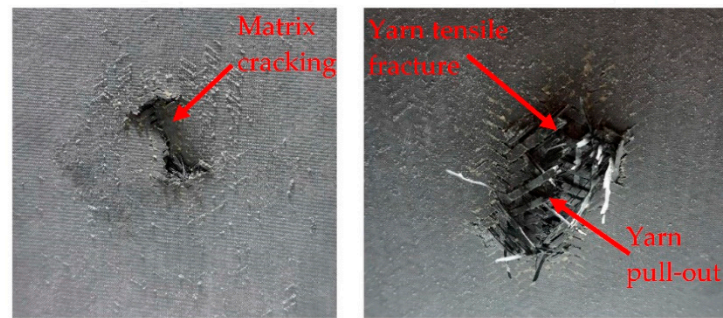
(a) H2, $V_i = 146$ m/s, $T = 143$ °C.



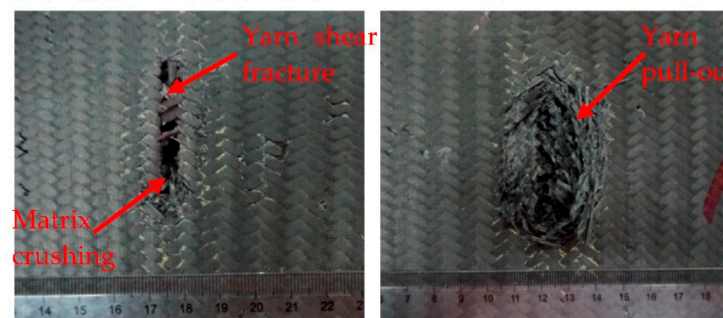
(b) H4, $V_i = 185$ m/s, $T = 149.5$ °C.

Figure 17. Damage to 2D triaxial braided composite target plate at high temperature due to impact of rectangular projectile.

Figure 18 shows an enlarged view of the local damage to the composite target at cryogenic and high temperatures. The images on the left (right) show the damage to the front (back) surface of the target. For tests at cryogenic conditions, damage at the impact surface consists of a tear opening with longitudinal and transverse cracks. The main failure modes of the target at the front surface are fiber fracture and matrix cracking. For tests at high temperature, the damage at the impact surface clearly differs from that at cryogenic conditions. A neat and complete rectangular perforation is caused by shearing. The main failure modes in this case are fiber shearing failure and matrix crushing failure.



(a) C3 test, 147 m/s, cryogenic temperature.



(b) H4 test, 185 m/s, high temperature.

Figure 18. Enlarged view of local perforation damage to 2D triaxial braided composite target at different temperatures.

Extensive yarn fracture and pull-out is evident at the exit surface. The tough fracture surface indicates that the yarn failure is the result of tensile forces. Matrix cracking and delamination failure are also significant failure modes at the target exit surface. Moreover, the extent of damage and the damage area of the target in test C3 are greater than in test C2. We presume that, at cryogenic temperatures, a greater incident velocity of the projectile correlates with greater damage and a larger damage area of the composite target plate, which differs from the result for metal blade-like projectiles (cf. Section 3.1.3 and previous studies [32]). For tests at high temperature, the exit surface consists of a rough fiber fracture surface with extensive yarn pull-out. The main failure forms are fiber tensile fracture, matrix cracking, and delamination failure, which is consistent with the results obtained at cryogenic temperature and room temperature.

4. Conclusions

The current study investigates the ballistic impact performance of 2D triaxial braided composite using three types of projectiles (gelatin cylindrical projectiles and CFRP and titanium-alloy blade-like projectiles) with similar masses and equivalent diameters for the casing containment application. Furthermore, impact tests of triaxial braided composites

were conducted at cryogenic and high temperatures considering the possible extreme working environment temperature. The current study aims to illustrate how projectile material and temperature affect the impact resistance of the composites. The main conclusions were drawn as follow:

- (1) Given the fluid behavior of gelatin projectiles under impact load, the triaxial braided composite target impacted with a gelatin projectile undergoes global deformation and therefore absorbs much more energy than when impacted by CFRP or titanium projectiles. Upon impact with a gelatin projectile, delamination, matrix cracking, and slight fiber breakage appear in the through-thickness direction of the target.
- (2) Triaxial braided composites impacted by CFRP and titanium-alloy blade-like projectiles produce similar damage patterns. A rectangular opening appears at the impact surface and an elliptically shaped damage area appears at the exit surface with massive fiber breakage, yarn pull-out, and severe matrix cracking and delamination. The average energy absorption of the triaxial braided composite when perforated by a CFRP projectile is 77.59% greater than that perforated by a titanium-alloy projectile. When the composite target is impacted by a titanium-alloy projectile, its main damage has a shear pattern, and barely global bending deformation occurs to dissipate energy. Therefore, the usage of composite fan blades is very important, because compared to titanium alloy blades, the application of composite blades could not only reduce the weight of the blade itself, but also further reduce the weight of the composite casing, which will bring enormous economic benefits.
- (3) Cryogenic temperatures deteriorate the impact resistance of 2D triaxial braided composite material while high temperature improves its impact resistance. This result is attributed mainly to the decreased flexibility of the 2D triaxial braided composite target plate at cryogenic temperature, which permits less global deformation under impact load. The temperature affects the damage pattern of the 2D triaxial braided composites. Therefore, in the design and analysis of the composite containment casing, it is necessary to consider the influence of the working environment temperature.

Author Contributions: Conceptualization, L.L. and W.C.; methodology, L.L. and S.Y.; software, Z.Z. and G.L.; validation, L.L. and S.Y.; formal analysis, S.Y.; investigation, L.L.; resources, G.L.; data curation, Z.Z.; writing—original draft preparation, S.Y. and L.L.; writing—review and editing, L.L.; visualization, Z.Z.; supervision, W.C.; project administration, W.C.; funding acquisition, L.L. and W.C. All authors have read and agreed to the published version of the manuscript.

Funding: This work was supported by the National Natural Science Foundation of China (Grant numbers 51975279 and 51605218) and the National Science and Technology Major Project [2017-IV-0006-0043].

Acknowledgments: The authors would like to thank undergraduate students Wang Yang and Liu Wenkui for the help in the testing procedure.

Conflicts of Interest: The authors declare no conflict of interest.

References

1. Khezri, M.; Rasmussen, K.J.R. An energy-based approach to buckling modal decomposition of thin-walled members with arbitrary cross sections, Part 1: Derivation. *Thin Wall. Struct.* **2019**, *138*, 496–517. [[CrossRef](#)]
2. Andrew, J.J.; Srinivasan, S.M.; Arockiarajan, A.; Dhakal, H.N. Parameters influencing the impact response of fiber-reinforced polymer matrix composite materials: A critical review. *Compos. Struct.* **2019**, *224*, 111007. [[CrossRef](#)]
3. Zhao, Z.; Dang, H.; Liu, P.; Guo, Z.; Zhang, C.; Li, Y. On the impact failure behavior of triaxially braided composites subjected to metallic plate projectile. *Compos. Part B Eng.* **2020**, *186*, 107816. [[CrossRef](#)]
4. He, Z.; Xuan, H.; Bai, C.; Song, M.; Zhu, Z. Containment of soft wall casing wrapped with Kevlar fabric. *Chin. J. Aeronaut.* **2019**, *32*, 954–966. [[CrossRef](#)]
5. Xuan, H.; Hu, Y.; Wu, Y.; He, Z. Containment Ability of Kevlar 49 Composite Case under Spinning Impact. *J. Aerosp. Eng.* **2018**, *31*, 04017096. [[CrossRef](#)]
6. He, Q.; Xie, Z.; Xuan, H.; Liu, L.; Hong, W. Multi-blade effects on aero-engine blade containment. *Aerosp. Sci. Technol.* **2016**, *49*, 101–111. [[CrossRef](#)]

7. He, Q.; Xuan, H.; Liu, L.; Hong, W.; Wu, R. Perforation of aero-engine fan casing by a single rotating blade. *Aerosp. Sci. Technol.* **2013**, *25*, 234–241. [[CrossRef](#)]
8. Shah, S.Z.H.; Karuppanan, S.; Megat-Yusoff, P.S.M.; Sajid, Z. Impact resistance and damage tolerance of fiber reinforced composites: A review. *Compos. Struct.* **2019**, *217*, 100–121. [[CrossRef](#)]
9. Dang, H.; Zhao, Z.; Liu, P.; Zhang, C.; Tong, L.; Li, Y. A new analytical method for progressive failure analysis of two-dimensional triaxially braided composites. *Compos. Sci. Technol.* **2020**, *186*, 107936. [[CrossRef](#)]
10. Zhao, Z.; Liu, P.; Chen, C.; Zhang, C.; Li, Y. Modeling the transverse tensile and compressive failure behavior of triaxially braided composites. *Compos. Sci. Technol.* **2019**, *172*, 96–107. [[CrossRef](#)]
11. García-Carpintero, A.; Van den Beuken, B.N.G.; Haldar, S.; Herráez, M.; González, C.; Lopes, C.S. Fracture behaviour of triaxial braided composites and its simulation using a multi-material shell modelling approach. *Eng. Fract. Mech.* **2018**, *188*, 268–286. [[CrossRef](#)]
12. Wehrkamp-Richter, T.; De Carvalho, N.V.; Pinho, S.T. A meso-scale simulation framework for predicting the mechanical response of triaxial braided composites. *Compos. Part A Appl. Sci. Manuf.* **2018**, *107*, 489–506. [[CrossRef](#)]
13. Jiang, H.; Ren, Y.; Liu, Z.; Zhang, S.; Yu, G. Multi-scale analysis for mechanical properties of fiber bundle and damage characteristics of 2D triaxially braided composite panel under shear loading. *Thin Wall. Struct.* **2018**, *132*, 276–286. [[CrossRef](#)]
14. Wehrkamp-Richter, T.; De Carvalho, N.V.; Pinho, S.T. Predicting the non-linear mechanical response of triaxial braided composites. *Compos. Part A Appl. Sci. Manuf.* **2018**, *114*, 117–135. [[CrossRef](#)]
15. Quek, S.C.; Waas, A.M.; Shahwan, K.W.; Agaram, V. Compressive response and failure of braided textile composites. Part 1: Experiments. *Int. J. NonLin. Mech.* **2004**, *39*, 635–648. [[CrossRef](#)]
16. Ivanov, D.S.; Baudry, F.; Van Den Broucke, B.; Lomov, S.V.; Xie, H.; Verpoest, I. Failure analysis of triaxial braided composite. *Compos. Sci. Technol.* **2009**, *69*, 1372–1380. [[CrossRef](#)]
17. Khosravani, M.R.; Anders, D.; Weinberg, K. Influence of strain rate on fracture behavior of sandwich composite T-joints. *Eur. J. Mech. A Solid* **2019**, *78*, 103821. [[CrossRef](#)]
18. Sutcliffe, M.P.F.; Aceves, C.M.; Stronge, W.J.; Choudhry, R.S.; Scott, A.E. Moderate speed impact damage to 2D-braided glass-carbon composites. *Compos. Struct.* **2012**, *94*, 1781–1792. [[CrossRef](#)]
19. Johnston, J.P.; Pereira, J.M.; Ruggeri, C.R.; Roberts, G.D. High-speed infrared thermal imaging during ballistic impact of triaxially braided composites. *J. Compos. Mater.* **2018**, *52*, 3549–3562. [[CrossRef](#)]
20. Barber, J.P.; Taylor, H.R.; Wilbeck, J.S. *Bird Impact Forces and Pressures on Rigid and Compliant Targets*; Technical Report AFFDL-TR-77-60; Air Force Flight Dynamics Laboratory: Wright-Patterson Air Force Base, OH, USA, 1978.
21. Barber, J.P.; Fry, P.F.; Klyce, J.M.; Taylor, H.R. *Impact of Soft Bodies on Jet Engine Fan Blades*; AFML-TR-77-29; University of Dayton Research Institute: Dayton, OH, USA, 1977.
22. Guan, Y.; Zhao, Z.; Chen, W.; Gao, D. Foreign Object Damage to Fan Rotor Blades of Aeroengine Part I: Experimental Study of Bird Impact. *Chin. J. Aeronaut.* **2007**, *5*, 408–414.
23. Liu, L.; Luo, G.; Chen, W.; Zhao, Z.; Huang, X. Dynamic behavior and damage mechanism of 3D braided composite fan blade under bird impact. *Int. J. Aerosp. Eng.* **2018**, *2018*, 5906078. [[CrossRef](#)]
24. Roberts, G.D.; Pereira, J.M., Jr.; Revilock, D.M.; Binienda, W.K.; Xie, M.; Braley, M. Ballistic impact of braided composite with a soft projectile. *J. Aerosp. Eng.* **2005**, *18*, 3–7. [[CrossRef](#)]
25. Cheng, J. Material Modeling of Strain Rate Dependent Polymer and 2D Triaxially Braided Composites. Ph.D. Thesis, Department of Civil Engineering, University of Akron, Akron, OH, USA, 2006.
26. Goldberg, R.K.; Blinzler, B.J.; Binienda, W.K. Modification of a Macromechanical Finite-Element Based Model for Impact Analysis of triaxially braided composites. *J. Aerosp. Eng.* **2012**, *25*, 383–394. [[CrossRef](#)]
27. Pereira, J.M.; Roberts, G.D.; Ruggeri, C.R.; Gilat, A.; Matrka, T. *Experimental Techniques for Evaluating the Effects of Aging on Impact and High Strain Rate Properties of Triaxial Braided Composite Materials*; NASA/TM—2010-216763; National Aeronautics and Space Administration, Glenn Research Center: Cleveland, OH, USA, 2010.
28. Liu, L.; Zhao, Z.; Chen, W.; Luo, G. Influence of pre-tension on ballistic impact performance of multi-layer Kevlar 49 woven fabrics for gas turbine engine containment systems. *Chin. J. Aeronaut.* **2018**, *31*, 1273–1286. [[CrossRef](#)]
29. He, Q.; Xie, Z.; Xuan, H.; Hong, W. Ballistic testing and theoretical analysis for perforation mechanism of the fan casing and fragmentation of the released blade. *Int. J. Impact Eng.* **2016**, *91*, 80–93. [[CrossRef](#)]
30. Pereira, J.M.; Revilock, D.M.; Ruggeri, C.R.; Emmerling, W.C.; Altobelli, D.J. Ballistic Impact Testing of Aluminum 2024 and Titanium 6Al-4V for Material Model Development. *J. Aerosp. Eng.* **2014**, *27*, 456–465. [[CrossRef](#)]
31. Zhang, T.; Chen, W.; Guan, Y.; Gao, D. Study on Titanium Alloy TC4 Ballistic Penetration Resistance. Part I: Ballistic Impact Tests. *Chin. J. Aeronaut.* **2012**, *25*, 388–395. [[CrossRef](#)]
32. Liu, L.; Zhao, Z.; Chen, W.; Shuang, C.; Luo, G. An experimental investigation on high velocity impact behavior of hygrothermal aged CFRP composites. *Compos. Struct.* **2018**, *204*, 645–657. [[CrossRef](#)]
33. Liu, L.; Xuan, H.; He, Z.; Niu, D.; Xing, J.; Hong, W. Containment capability of 2D triaxial braided tape wound composite casing for aero-engine. *Polym. Compos.* **2016**, *37*, 2227–2242. [[CrossRef](#)]
34. Xuan, H.; Liu, L.; Chen, G.; Zhang, N.; Feng, Y.; Hong, W. Impact response and damage evolution of triaxial braided carbon/epoxy composites. Part I: Ballistic impact testing. *Text. Res. J.* **2013**, *83*, 1703–1716.

35. Liu, L.; Xuan, H.; Zhang, N.; Chen, G.; Feng, Y.; Hong, W. Impact response and damage evolution of triaxial braided carbon/epoxy composites. Part II: Finite element analysis. *Text. Res. J.* **2013**, *83*, 1821–1835.
36. Liu, L.; Xuan, H.; Chen, W.; Zhao, Z.; Guan, Y. Modified Subcell Model Using Solid Elements for Triaxial Braided Composite under Ballistic Impact. *J. Aerosp. Eng.* **2016**, *29*, 04016028. [[CrossRef](#)]
37. Tan, H.; Liu, L.; Guan, Y.; Chen, W.; Zhao, Z. A simplified delamination modelling methodology for triaxial braided composites with macro-scale solid finite-element models. *Int. J. Crashworthines.* **2019**, *24*, 54–70. [[CrossRef](#)]
38. Zhao, Z.; Dang, H.; Zhang, C.; Yun, G.; Li, Y. A multi-scale modeling framework for impact damage simulation of triaxially braided composites. *Compos. Part A Appl. Sci. Manufact.* **2018**, *110*, 113–125. [[CrossRef](#)]
39. Miller, S.G.; Handschuh, K.M.; Sinnott, M.J.; Kohlman, L.W. *Materials, Manufacturing, and Test Development of a Composite Fan Blade Leading Edge Subcomponent for Improved Impact Resistance*; NASA/TM—2015-218340; National Aeronautics and Space Administration, Glenn Research Center: Cleveland, OH, USA, 2015.
40. Amoo, L.M. On the design and structural analysis of jet engine fan blade structures. *Prog. Aerosp. Sci.* **2013**, *60*, 1–11. [[CrossRef](#)]
41. Ridzuan, M.J.M.; Majid, M.S.A.; Khasri, A.; Basaruddin, K.S.; Gibson, A.G. Effect of moisture exposure and elevated temperatures on impact response of Pennisetum purpureum/glass-reinforced epoxy (PGRE) hybrid composites. *Compos. Part B Eng.* **2019**, *160*, 84–93. [[CrossRef](#)]
42. Sorrentino, L.; de Vasconcellos, D.S.; D’Auria, M.; Sarasini, F.; Tirillò, J. Effect of temperature on static and low velocity impact properties of thermoplastic composites. *Compos. Part B Eng.* **2017**, *113*, 100–110. [[CrossRef](#)]
43. Wang, Y.; Zhang, J.; Fang, G.; Zhang, J.; Zhou, Z.; Wang, S. Influence of temperature on the impact behavior of woven-ply carbon fiber reinforced thermoplastic composites. *Compos. Struct.* **2018**, *185*, 435–445. [[CrossRef](#)]
44. Khashaba, U.A.; Othman, R. Low-velocity impact of woven CFRE composites under different temperature levels. *Int. J. Impact Eng.* **2017**, *108*, 191–204. [[CrossRef](#)]
45. Amaro, A.M.; Reis, P.N.B.; Neto, M.A. Experimental study of temperature effects on composite laminates subjected to multi-impacts. *Compos. Part B Eng.* **2016**, *98*, 23–29. [[CrossRef](#)]
46. Sreekantha Reddy, T.; Rama Subba Reddy, P.; Madhu, V. Low velocity impact studies of E-glass/epoxy composite laminates at different thicknesses and temperatures. *Def. Technol.* **2019**, in press. [[CrossRef](#)]
47. Ma, H.; Jia, Z.; Kintak, L.; Leng, J.; Hui, D. Impact properties of glass fiber/epoxy composites at cryogenic environment. *Compos. Part B Eng.* **2016**, *92*, 210–217. [[CrossRef](#)]
48. Shimamoto, A.; Kubota, R.; Takayama, K. High-velocity impact characteristic of carbon fiber reinforced plastic composite at low temperature. *J. Strain Anal. Eng.* **2012**, *47*, 471–479. [[CrossRef](#)]
49. Mohammad, R.K. Composite Materials Manufacturing Processes. *Appl. Mech. Mater.* **2011**, *110–116*, 1361–1367.
50. Anderson, C.E., Jr.; Hohler, V.; Walker, J.D.; Stilp, A.J. The influence of projectile hardness on ballistic performance. *Int. J. Impact Eng.* **1999**, *22*, 619–632. [[CrossRef](#)]
51. Luo, G.; Xu, Z.; Shen, H.; Chen, W.; Zhang, H. Experimental study on the impact load of internally supported gelatin bird projectiles. *Eng. Fail. Anal.* **2021**, *124*, 105336. [[CrossRef](#)]